

Response of *Vallisneria natans* to aluminum phytotoxicity and their synergistic effect on nitrogen, phosphorus change in sediments

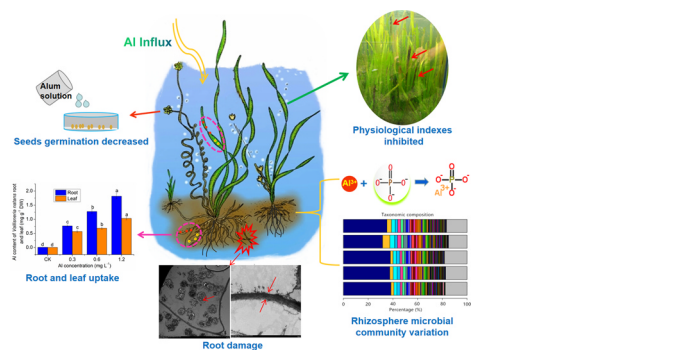
Qingwei Lin^{a,b}, Mingjun Fan^a, Xue Peng^b, Jianmin Ma^a, Yi Zhang^b, Fei Yu^a, Zhenbin Wu^b, Biyun Liu^{b,*}

^a College of Life Sciences, Henan Normal University, Xinxiang, 453007, China

^b State Key Laboratory of Freshwater Ecology and Biotechnology, Institute of Hydrobiology, Chinese Academy of Sciences, Wuhan, 430072, China



GRAPHICAL ABSTRACT



ARTICLE INFO

Editor: Rinklebe Jörg

Keywords:

Aluminum phytotoxicity
Microorganisms community
Nitrogen phosphorus nutrient
Sediment
Vallisneria natans

ABSTRACT

Increasing aluminum (Al) use and its effects on aquatic systems have been a global issue, however the Al impacts on submerged plants and their ecological functions were poorly understood. Aquatic simulation experiments were performed to study Al-toxicity on the germination and seedling morphological and physiological characteristics of *Vallisneria natans*, and investigate their synergistic effect on nitrogen (N), phosphorus (P) change and microbial community in sediment. The seeds germination characteristics, growth and physiological parameters of seedlings, including root activity, were significantly affected by alum treatments and the inhibition levels increased with Al³⁺ concentration. The Al accumulation in roots and leaves were significantly different. Al³⁺ concentration above 0.3 mg/L showed toxic to *V. natans*. TN, TP, IP, Fe/Al-P contents in sediments varied markedly under co-existence of Al and *V. natans*. Additionally, the relative abundance of sediment microbial community related to N, P cycle was effected. Results concluded that the increasing aquatic Al-concentration inhibits growth and propagation of submerged plants and the ecological restoration effect, and exerts synergistic effect with submerged plants on N, P components in sediments. Such findings were helpful for Al ecological evaluation, and were instructive for the submerged plants restoration in shallow eutrophic lakes with Al input.

* Corresponding author.

E-mail address: liuby@ihb.ac.cn (B. Liu).

1. Introduction

The widely utilization of Al, the most abundant metallic element on earth, in manufacturing, food, medicines and electronic materials has been well-documented (Tsakiridis, 2012; Patrick et al., 2019). Past few decades have also witnessed diverse Al inpouring into aquatic ecosystems as a consequence of anthropogenic or/and natural activities (Cooke et al., 2005), including the commonly application of Al-based flocculation agents in the wastewater treatment and controlling nuisance algal blooms in eutrophic lakes (Reitzel et al., 2005). Sediment Al content in European and North American lakes had reached 2.916–38.286 g/kg DW (Kopacek et al., 2005). And Al concentrations in groundwater and surface water are reported 140–290 ug/L and 16–1170 ug/L, respectively, in the U.S.A. (Robert and Richard, 1999). Increasing Al concentrations in aquatic habitats has been a global issue (Adams et al., 2018; Patrick et al., 2019).

In aquatic ecosystems, free metal ion Al^{3+} , can form amorphous $\text{Al}(\text{OH})_3$ flocs by hydrolysis reaction. Phosphate could be captured and combined with flocs-particles to precipitate forming a passive layer on sediment, which prevent endogenous phosphorus (P) release (Cooke et al., 2005; Huser et al., 2016), and the complexation with Al-salts reduced P phyto-availability (de Vincente et al., 2008; Lin et al., 2017a). Due to the chelate effect between Al-salts with certain nitrogenous groups, significant relationships were confirmed between Al and nitrogen (N), depending on the environmental physico-chemical conditions in sediment (Lin et al., 2019).

Previous Al-toxicity studies have mostly focused on the terrestrial plants (Ma et al., 2014; Yu et al., 2015; Kochian et al., 2015), verifying that under acidic conditions, the activated Al^{3+} restrict crop yields and lead to forest decline (Robert and Richard, 1999). Al stress can impact plants root elongation and cytoskeleton (He et al., 2017), physiological/biochemical response (Dawood et al., 2012; Robert et al., 2018) and nutrient biological availability. Additionally, Al can also damages the microorganisms cell structures, inhibits their material and energy metabolism, affects their growth and development (Dorea and Clarke, 2008), ultimately changes the specific composition and community structure (Wang, 2010). Al entering into the water bodies are likely to influence aquatic organisms for continuous accumulation, while the Al-toxicity study on submerged macrophytes was yet extremely scarce, though having scanty and superficial studies on *Potamogeton crispus* (Lin et al., 2017b), *Hydrilla verticillata* (Lin et al., 2017c), *Najas guadalupensis* (Lynette et al., 2010). The study of Al-phytotoxicity on submerged macrophyte and their synergistic effect on submerged macrophyte ecological restoration is therefore extremely urgent and significant in aquatic system of eutrophication.

Eutrophication and ecosystem degradation of water bodies caused by human activities and global climate change are important water environment problems worldwide (Morelli et al., 2018). At present, the macrophyte vegetation restorations are still significant for control eutrophication and ecological function-improving of degraded aquatic ecosystem (Xing et al., 2013). Submerged plants contribute greatly in the restoration, which improving productivity, stabilizing sediment, reducing N and P nutrients loads, but also change the distribution and community structure of sediment microorganisms (Lynette et al., 2010). During the restoration, seeds culture and seedlings transplant are primarily applied. While the Al accumulation in water body may be injurious even destructive influence on the seed germination and growth of submerged plants. N, P were also utilized by submerged plants, but the Al-induced P low-availability and acid phosphatase enzyme inhibition (Ziaeи et al., 2014) leads to plant growth-inhibiting and biomass-limiting (Chaudhary et al., 2008; Vieira et al., 2008). In this case, however the synergistic effects of Al and the aquatic macrophyts on the N, P fractions or vice versa remains unclear.

Submerged plants utilize N and P nutrients both in water columns and sediments to grow. Meanwhile, the normal growth process of submerged plants will regulate the oxygen content in the sediments

through radial oxygen loss, combining with the root exudates of submerged plants, thus optimize the rhizospheric microbial community structure, which affects the transformation of N and P in the sediments (Cooke et al., 2005; Lynette et al., 2010). Submerged plants have a certain response to environmental stress, such as N and P nutrient deficiency, heavy metal pollution, organic pollution etc. (Xing et al., 2013; Ziaeи et al., 2014), involving the changes of photosynthetic pigments, free proline and the decrease of root activity (Ziaeи et al., 2014; Lin et al., 2017b). But the studies on the stress of Al phytotoxicity on the submerged plants are limited.

Vallisneria natans, one dominated submerged species in many aquatic systems, was primarily used in ecological restoration because strong ability of bearing dirty, high breeding ability and with a vast range of distribution (Zuo et al., 2016; Yu et al., 2017). The reproduction and community development of *V. natans* mainly depends on sexual reproduction of seeds and asexual propagation of tubers and stolons. Many environmental factors, e.g. nutrient level, sediment properties, illumination, heavy metals, have been reported to determine the fate of *V. natans* (Lin et al., 2017c; Yu et al., 2017; Wang et al., 2018b). While the influence of Al contaminant on *V. natans* restoration has been little studied.

On above basis, we conducted a multi-dose experiment on the phytotoxic response of *V. natans* to alum solution, the aims were (1) to determine whether Al-salt could affect the seeds germination and seedlings physiological characteristics, (2) to investigate the aquatic-phytotoxic effect and mechanism of Al-salt and its accumulation characteristics in *V. natans*, (3) to explore the synergistic effect of Al and *V. natans* on rhizospheric N, P content change and microflora community trends. The findings will be important guidelines for the ecological restoration of submerged macrophytes in shallow eutrophic lakes with Al input, and for the ecological evaluation and scientific utilization of Al-salts.

2. Materials and methods

2.1. Preparation of aluminum salt and submerged macrophyte

Al contamination was achieved using alum ($\text{KAl}(\text{SO}_4)_2 \cdot 12\text{H}_2\text{O}$) (Analytic pure level) solution in triplicates, which was prepared to 10 mg/L Al^{3+} mother liquor.

V. natans seedlings were cultivated by seeds, which were purchased from Gaochun Futian Aquatic Macrophyte Company (Nanjing, China). Plump seeds, that pre-soaked for 10 h, were selected and cultured into plastic basins ($10 \times 10 \times 10$ cm, 50 cm × 25 cm × 20 cm) containing sediments (7 cm depth) and water. The seeds were then cultured in lab under natural conditions. The growth-consistent *V. natans* seedlings (10.0 ± 0.2 cm) were selected for subsequent Al-exposure experiment. Aquariums (25 cm × 25 cm × 50 cm) were applied to establish the aquatic controllable microcosm.

2.2. Mesocosms set up: effect of Al on seeds germination of *V. natans*

V. natans seeds were germinated in Petri dishes (12 cm Φ, 2 cm H) where paved two bibulous papers. Alum solutions with different Al^{3+} concentrations (0 mg/L (CK), 0.3 mg/L, 0.6 mg/L and 1.2 mg/L) were prepared and added into 1/10 Hoagland's culture solution to achieve Al-salts culture solutions (ACS).

100 seeds were cultured onto the bibulous paper space-evenly with 50 mL ACS, according to Ke and Li (2006). 20 mL ACS was supplemented every 2 days to avoid evaporation loss. A seed was considered to have germinated when the radicle emerged from the seed coat. Afterwards, the relevant indexes, such as the germination rate (G_r), germination viability (G_v), germination index (G_i) were calculated, according to the method by Wei et al. (2013).

2.3. Mesocosms set up: effects of Al on the seedling morphological and physiological characteristics of *V. natans*

Surface sediments that collected from Jinshagang Lake, Hangzhou, where no foreign Al contamination, after removal of impurities and adequately blending, were tiled in aquariums 15 cm depth. The physicochemical properties of sediments: organic matter (OM) content was 10.13 %, redox potential (Eh) was 248.27 mv, TN 6.880 mg/g, TP 1.459 mg/g, IP 1.281 mg/g, Fe/Al-P 0.605 mg/g, Ca-P 0.808 mg/g, and the moisture content 43.89 %.

Five groups of aquariums were set up (three repetitions): (1) NO: sediments + tap water, (2) CK: sediments + tap water + *V. natans*, (3) 0.3: sediments + tap water + *V. natans* + 0.3 mg/L Al³⁺ alum solution, (4) 0.6: sediments + tap water + *V. natans* + 0.6 mg/L Al³⁺ alum solution, (5) 1.2: sediments + tap water + *V. natans* + 1.2 mg/L Al³⁺ alum solution. 16 plants of *V. natans* seedlings were planted into each aquarium. Five days after Al contamination, one *V. natans* plant in each parallel was sampled and the roots were put into electron microscope scanning and root activity assay analysis. In the end of experiment, *V. natans* were harvested carefully then measured involve in morphological and physiological indicators.

2.4. Water and sediment analysis

Water TN and TP were determined using the alkaline potassium persulfate digestion ultraviolet spectrophotometric method and potassium persulfate digestion ammonium molybdate spectrophotometric method respectively (Yu et al., 2017) with a ultraviolet/visible specturm spectrophotometer (JINGHUA-752 N, Shanghai, China). Water Al concentration was determined using inductively coupled plasma-atomic emission spectrometry (ICP-AES).

The sediment Al content was measured after 5–6 h microwave digestion using a mixture solution (10 mL, v:v = 20:1) of nitric acid and hydrofluoric acid (Aladdin, Shanghai, Semiconductor Grade) under 160 °C condition, and determined with ICP-AES (Optima 2000 DV, PerkinElmer). The limit of quantification was 0.001 g/kg DW.

The total nitrogen (TN) content of sediment was determined by the method described by Lin et al. (2019). And the content of the P fraction, including total P (TP), inorganic P (IP), organic P (OP), Fe/Al-P and Ca-P, were measured following the SMT protocol (Ruban et al., 2001).

2.5. *V. natans* sampling, morphological and physiological parameters measurement

V. natans were carefully harvested with the whole roots system, and collected into portable refrigerator after impurities removing. *V. natans* samples were firstly classified into three parts, namely, the roots, stolon and leaf, then their biomass were determined respectively. The ratio of underground : above ground biomass was determined by the biomass of (roots + stolons) / the biomass of leaves. The clonal ramets number, stolons number and stolon length were calculated. 50 roots of each treatment were randomly selected and soaked, straightened on microscope slide, then root diameter was measured by micrometer of microscope.

The chlorophyll contents of *V. natans* seedlings were extracted from 0.2 g leaves using 25 mL of 95 % alcohol at room temperature. The concentrations of chlorophyll-a (Chl-a), chlorophyll-b (Chl-b), and carotene were determined spectrophotometrically at 665 nm, 649 nm, and 470 nm (JINGHUA-752 N, Shanghai, China) and calculated (Lin et al., 2017b). The ascorbic acid (AsA) content was assayed using trichloroacetic acid (TCA)-spectrophotometric method (Zhou et al., 2016). Free proline was determined according to the sulfosalicylic acid extraction - ninhydrin colouring method described by Patricia and Manuela (2016).

2.6. Al localization and P content in roots and leaves

At the end of Al contamination, the roots were washed with double distilled water (DDW), and 1 cm apical portions (including the root cap) were cut using a razor blade. The excised root apices (four replicate segments) were transferred to 1.5 mL Eppendorf (Netheler-Hinz, GmbH, Hamburg, Germany) tubes where containing 1 mL of 2 M HCl for 48 h. The Al content in the HCl digests was determined by an atomic absorption spectrophotometer (Z-8270, Hitachi, Tokyo, Japan) after dilution.

The dried roots samples were digested by HNO₃ and HClO₄, then the P content in roots were measured using atomic absorption spectrophotometer after dilution and calculated.

2.7. Al-toxicity on root apices

The root activity was estimated by the triphenyltetrazolium chloride (TTC) reaction and ethyl acetate extraction method (Lin et al., 2017b).

Besides, the roots were cleaned for 5 min in DDW, stained with 10 mM MES [2-(N-morpholino) ethanesulphonic acid] buffer (pH 5.5) containing 100 u M Morin (Sigma, Tokyo, Japan) for 30 min, then the robust root tips were selected and cut 2–3 mm from the roots top with a razor blade. Afterwards, the cut tips were prepared into observation samples after complex processes involving pretreatment, embedding, ultra-thin sections. The ultrastructure of cells in the cross-section surface of the roots was observed by transmission electron microscope (HT-7700, Hitachi, Japan), and the images were obtained using a Zeiss confocal microscope (Axioplan 2 connected with LSM 510, Carl Zeiss, Oberkochen, Germany) at 488 nm excitation wavelength.

2.8. Rhizosphere microorganisms community

Total genome DNA from *V. natans* roots sediment samples was extracted using CTAB/SDS method. 16S rRNA genes of distinct regions were amplified used specific primer with the barcode. After mixed in equidenity ratios, the polymerase chain reaction (PCR) products was purified with GeneJETTM Gel Extraction Kit (Thermo Scientific). Sequencing libraries were generated using Ion Plus Fragment Library Kit 48 rxns following manufacturer's recommendations. The library was sequenced on an Ion S5 TM XL platform and 400 bp/600 bp single-end reads were generated.

Then, OTUs (Operational taxonomic units) clustering and species classification analysis were carried out based on the available data, and abundance, diversity index. Meanwhile, the community structure was statistically analyzed on each classification level of species annotation. The diversity index of microbial community in rhizosphere was calculated according to the following formula: OTU, the sequence of microbial samples after sequencing was clustered according to distance, and the original sequence was divided into multiple sequences according to sequence similarity. Each aggregation was an OTU.

$$H_{\text{shannon}} = - \sum_{i=1}^{S_{\text{obs}}} \frac{n_i}{N} \ln \frac{n_i}{N} \quad (1)$$

$$D_{\text{simpson}} = \frac{\sum_{i=1}^{S_{\text{obs}}} n_i (n_i - 1)}{N(N - 1)} \quad (2)$$

Where, S_{obs} is the number of OTU actually observed; n_i is the number of sequences contained in the OTU; N is the number of all individuals, in this case the total number of sequences.

2.9. Statistical analysis

Figures were prepared using Origin 8.0. Differences in the growth morphological and physiological parameters of *V. natans* under Al effects were compared using One-way analysis of variance (ANOVA) with

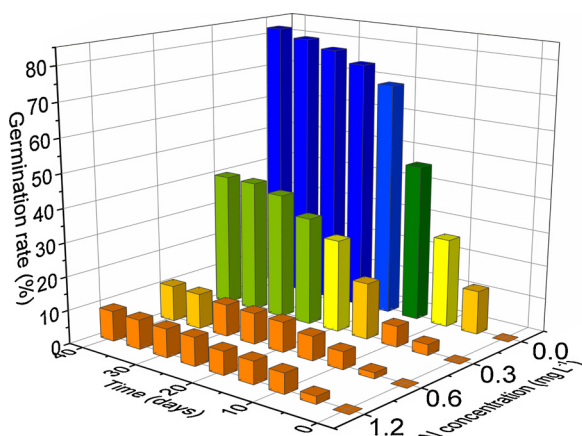


Fig. 1. The germination rate of *V. natans* seeds under different concentration of Al.

means separation by Duncan's test using SPSS 21 software at a significance level of $P < 0.05$. Furthermore, multiple comparisons of means were performed through LSD at the 0.05 significance level to identify differences among treatments.

3. Results and discussion

3.1. The germination rate, germination viability and germination index

The germination characteristics of *V. natans* seeds, including G_r , G_v and G_i , were verified to be significantly reduced by alum treatments ($P < 0.05$, Fig. 1, Table 1). The maximum values of the G_r during the experiment process were invariably located in the control groups. The G_r decreased markedly with the Al concentration increasing. The seeds started germinated on the 4th day in control and 5th day in other treatment. The G_r of 10th day in control groups, 0.3 mg/L, 0.6 mg/L and 1.2 mg/L treatments were respectively 26.50 %, 6.25 %, 5.25 % and 6.00 %, and the final G_r were 82.25 %, 39.75 %, 10.75 % and 9.00 %, with significantly differences among the four treatments except for 0.6 mg/L and 1.2 mg/L treatments. The highest G_v (82.25 %) and the highest G_i (21.76) were presented in control groups, and there were significant differences among control groups and treatments.

The phytotoxic action of Al on *V. natans* seeds altered the germination process, being similar to the toxicity on the terrestrial plants, mainly because of the hormonal imbalance of starch, soluble sugar and protein in seeds (Robert et al., 2018). The combination of Al^{3+} with the $-SH$, $-NH_2$ and $-COOH$ in starch, soluble sugar and protein also reduced these organic nutrients' bioavailability (Ma et al., 2014). More importantly, Al-toxicity compromise the plant seeds embryo development through endosperm cell destruction and solute extrusion (Ke and Li, 2006).

Different letters indicate significant differences ($P < 0.05$) among the four treatments. Data represent Means \pm S.E. n=3.

3.2. The *V. natans* morphological characteristics

The biomass and the average plant height exhibited regular reduction with the Al concentration increase ($P < 0.05$, Fig. 2). However, the root weight and plants number were the least in 0.6 mg/L Al^{3+}

treatment among the CK groups and treatments. In addition, the minimum value of the ratio of underground / above-ground biomass (0.222) was also in 0.6 mg/L treatment. This may be one strategy to adapt to Al inhibition, and it also confirms that the toxic target organ of Al-salt on plants is the root system. Visually, *V. natans* leaves in 1.2 mg/L Al^{3+} treatment showed darkening and wilting on the 10th day of the experiment. Al^{3+} highly likely destroyed the cell wall structure, more water entered the cell and resulted in necrosis of *V. natans* leaf tissue. Toxic effects of Al on submerged plant *P. crispus* have also been observed, with a 26.1–82.5 % decrease in biomass and 66.0–93.8 % decrease in root weight (Lin et al., 2017b). The root growth and development could be constrained primarily by Al toxicity (Poschenrieder et al., 2008). This suggested that Al compromises root and plant growth of *V. natans*, resulting in seedlings with less biomass and plant height, as observed in the present study.

3.3. Chlorophyll, ascorbic acid, free proline content and root activity

The physiological parameters of *V. natans* were significantly influenced by alum treatment ($P < 0.05$, Fig. 3). Although the maximum carotene content (0.141 mg/g FW) was present in 0.6 mg/L treatment, the maximum amounts of Chl-a and Chl-b content were all observed at CK groups (0.663, 0.297, 0.960 mg/g FW, respectively) (Fig. 3A). Al could cause deficiencies in Ca^{2+} and Mg^{2+} as well as other physiological stresses for plants (Collignon et al., 2012). Al may also compete with Mg^{2+} in chromatophores (Charlotte et al., 2008), subsequently inhibiting photosynthetic electron transport, so synthesis potential of photosynthetic pigment goes down (Ziaeи et al., 2014). The most obvious phenomenon was the yellowing of *V. natans* leaves in the 1.2 mg/L treatment.

In general, AsA is positively correlated with the resistance of plants (Bulley and Laing, 2016), and plays multiple roles in metabolic function and antioxidation effect (Akram et al., 2017). Although the AsA contents increased relative to the control groups within the concentration range of 0.6 mg/L, but no significant differences were found among CK groups, 0.3 mg/L and 0.6 mg/L treatments ($P > 0.05$) (Fig. 3B). The AsA content showed a noteworthy reduction in 1.2 mg/L treatment (0.118 mg/g FW), suggesting a weaker metabolic function for Al poisoning and the unbalance of mediating oxidative stresses resulted from Al-toxicity (Akram et al., 2017).

Additionally, it was verified an increase proline content in all Al^{3+} concentration treatments in comparison to CK groups, there was significant difference between the CK groups and 1.2 mg/L treatment (14.558 ug/g FW) (Fig. 3C). Free proline accumulation may contribute to stress resistance, by osmotic adjustment at cellular level and enzyme protection stabilizing the structure of macromolecules and organelles (Ziaeи et al., 2014; Talebi et al., 2014). The increasing generation of free proline indeed indicated the more stress from Al-toxicity for *V. natans* with Al^{3+} concentration increase, being similar to *Lactuca sativa* L (Patricia and Manuela, 2016).

Root activity linearly decreased with Al^{3+} concentration, and the statistical difference were significant among CK groups and treatment groups ($P < 0.05$, Fig. 3D). The transition zone of root apex is the most Al sensitive part (Poschenrieder et al., 2008; Chen et al., 2014). Al interaction with the apical root zone inhibits the cell elongation and division in the apical root meristem within minutes (Doncheva et al., 2005). By binding with enzyme proteins and genetic material in root cells, Al^{3+} could inhibit enzyme activity and prevent DNA replication,

Table 1

The germination viability and germination index under different concentration of Al.

	0mg/L	0.3mg/L	0.6mg/L	1.2mg/L
Germination viability	82.25 ± 3.42^a	39.75 ± 2.84^b	10.75 ± 0.85^c	9.00 ± 0.91^c
Germination index	21.76 ± 1.61^a	8.43 ± 0.79^b	3.06 ± 0.50^c	2.95 ± 0.48^c

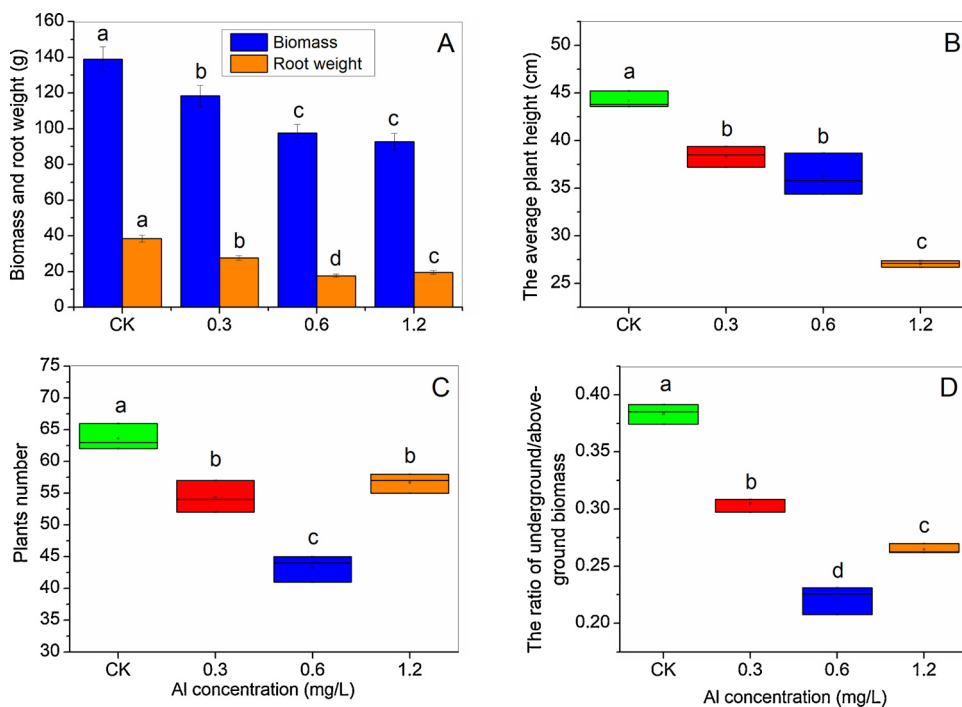


Fig. 2. The morphological parameters of *V. natans* (Different letters indicate significant differences ($P < 0.05$) among CK and the treatments. Data represent means \pm S.E. $n = 3$.).

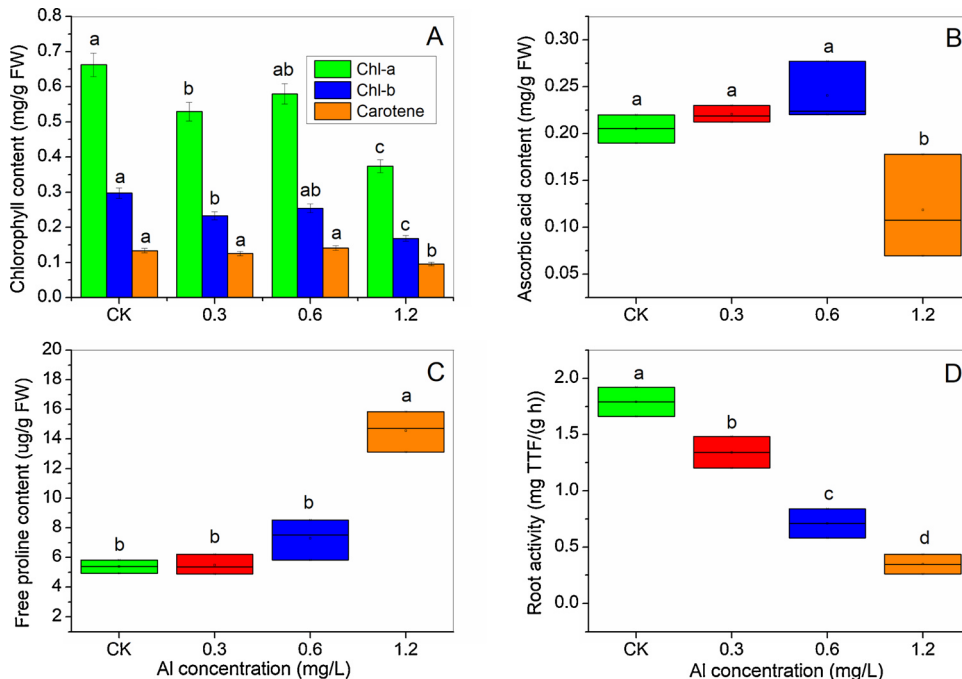


Fig. 3. Chlorophyll content (A), ascorbic acid content (B), free proline content (C), and root activity (D) of *V. natans* (Different letters indicate significant differences ($P < 0.05$) among CK groups and the treatments. Data represent means \pm S.E. $n = 3$.).

eventually affect the normal physiological process of roots (Yamamoto et al., 2002; He et al., 2017). The concentration $> 0.3 \text{ mg/L Al}^{3+}$ treatments caused toxic effect on roots, so the energy required for root metabolism could not be produced properly.

3.4. The cellular structure in root apex

The primary and most dramatic symptom of Al phytotoxicity is inhibition of root growth, involving root cell division, root elongation,

and roots generation, etc. (He et al., 2017). The current destruction symptoms intuitively proved that Al-salt had a toxic effect on the structure of the root apex cells in *V. natans* (Figs. 4, 5). The cells in the CK groups showed complete structures and complete intracellular organelles. The cell wall in 0.3 mg/L treatment appears to be thickened, which may be a moderate response or initial damage change after Al stress. While in the 0.6 mg/L treatment the cytoplasm was destroyed or disappeared, and only obvious cell wall or plasma membrane structure was observed (Fig. 4C-1, C-2). A stunted root system with functionally

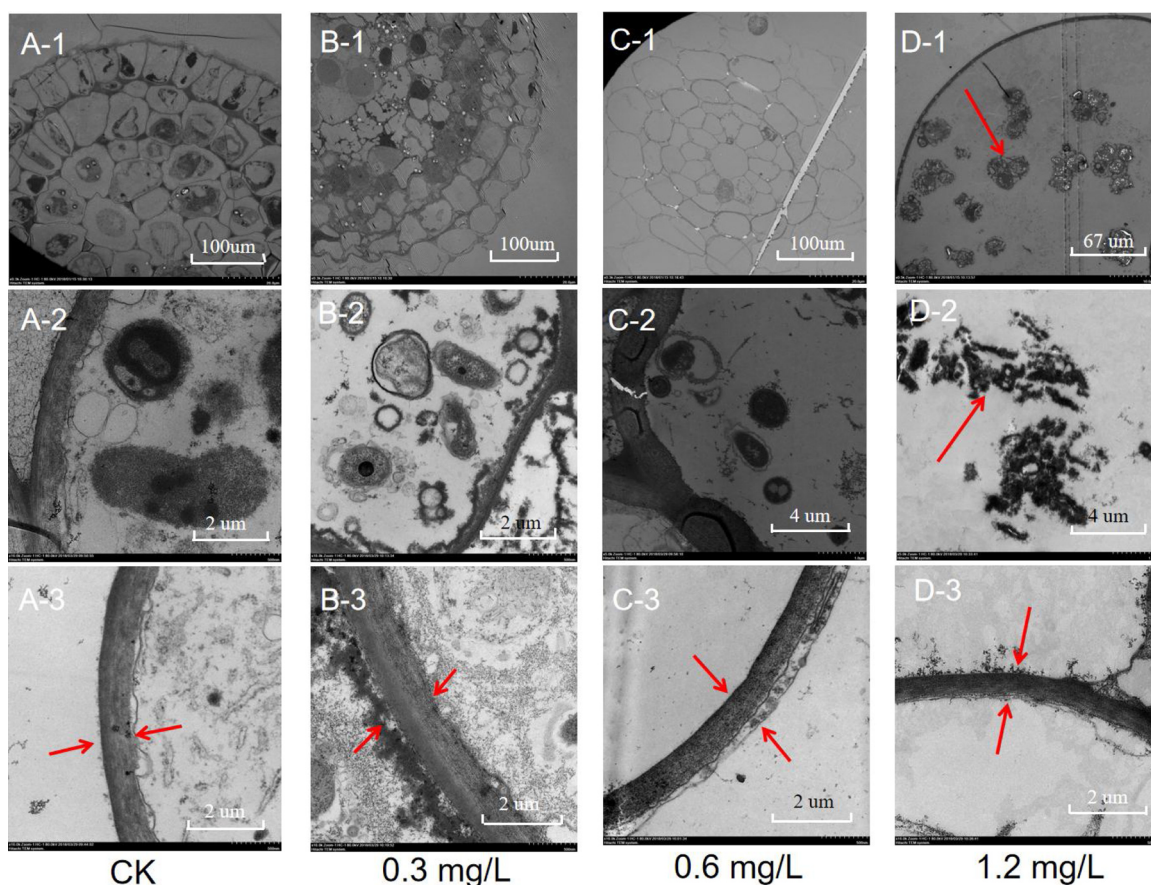


Fig. 4. Electron microscopy images of the root apices of *V. natans* (A-1, B-1, C-1 and D-1 respectively represented the whole image of CK groups, 0.3 mg/L, 0.6 mg/L and 1.2 mg/L Al^{3+} treatments. A-2, B-2, C-2, D-2 respectively showed the specific parts of CK groups, 0.3 mg/L, 0.6 mg/L and 1.2 mg/L Al^{3+} treatments. A-3, B-3, C-3, D-3 respectively indicated the lateral surface cell wall structure of CK groups, 0.3 mg/L, 0.6 mg/L and 1.2 mg/L Al^{3+} treatments).

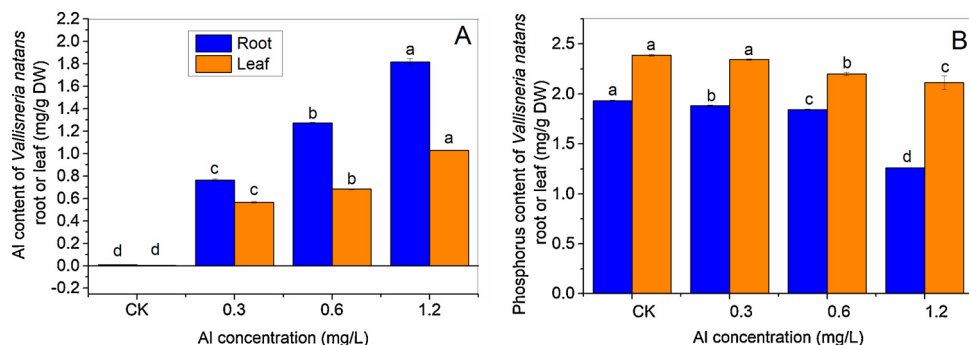


Fig. 5. Aluminum (A) and phosphorus content (B) in roots and leaves of *V. natans* (Different letters indicate significant differences ($P < 0.05$) among CK groups and the treatments. Data represent means \pm S.E. $n = 3$).

degraded cells is generally the consequence of early Al toxicity events (Doncheva et al., 2005). In the 1.2 mg/L treatment, the cell structure was severely damaged, the cell wall and plasma membrane, the organelle structure were blurred or even not observed. Al^{3+} is easily to bind with lipids and lipoproteins in the plasma membrane, and destroy its structure and ion channel (Kochian, 1995). Additionally, Al^{3+} can combine with the colloid, protein and other components of plant somatic cell wall, reducing the elasticity and conductivity of cell wall (Kochian et al., 2004). So dense amorphous cells were produced in the cells, and white substances were secreted and accumulated, which might be the amyloid in the root crown cells (Fig. 4D-1, D-2).

3.5. Al localization and P content in roots and leaves

Al and P accumulation in roots and leaves were significantly influenced by alum treatment ($P < 0.05$, Fig. 5). The Al accumulation in both *V. natans* seedling roots and leaves increased with adding Al concentration, and among the CK groups and treatment groups existed significant differences ($P < 0.05$). Al content ranged from 0.009 to 1.815 mg/g DW in roots, which were greater than that in leaves (0.004–1.030 mg/g DW). This indicated that *V. natans* could absorb Al by both roots and leaves, the primary way of Al entering plants is through the root system and the absorbed Al was mainly distributed in the roots, so the symptoms of Al-toxicity first appeared in the root system.

P content in roots and leaves decreased with the adding Al

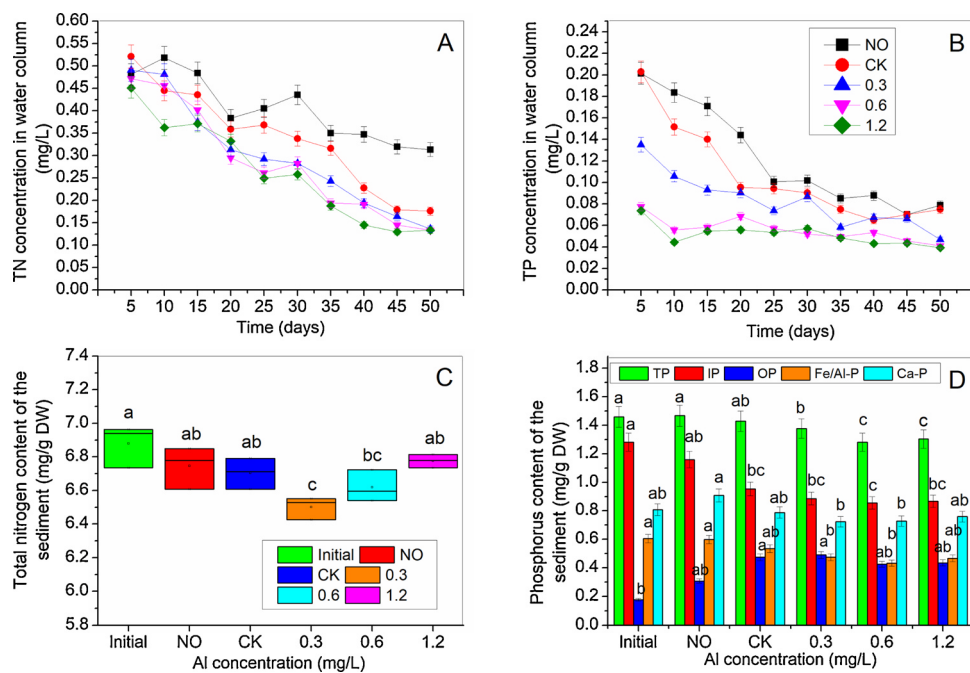


Fig. 6. The TN concentration (A) and TP concentration (B) in water column and TN content in sediment (C), phosphorus fractions content in sediment (D) (Different letters indicate significant differences ($P < 0.05$) among the treatments. Data represent means \pm S.E. $n=3$).

concentration, and the P content in roots were 1.262–1.933 mg/g DW, which was lower than that in the leaves (2.113–2.386 mg/g DW). This was related with the *V. natans* roots damage or the decrease of the biological availability of P for the P-passivation by Al-salt. Analytically significant differences were observed for P content in roots among CK groups and treatment groups ($P < 0.05$). This displayed that Al reduces P uptake rates by suppressing the activity of acid phosphatase enzyme and influencing the utilization of internal polyphosphate bodies in plants (Robert and Richard, 1999; Ma et al., 2014).

3.6. N, P content change in water and sediment

The *V. natans* planting and Al-salt addition exerted a synergistic effect on the concentration reduction of TN and TP in experimental systems. TN and TP concentrations were highest in NO groups, following with CK groups, and lowest in 1.2 mg/L treatment (Fig. 6A, B), this may because the function of plant absorption and assimilation in CK groups, while the combined effects of plant absorption/assimilation and Al-salts bonding with substances related with N, P occurred in treatment groups.

TN content in the NO groups sediments decreased slightly comparing with the initial value, which may mainly due to the function of microorganisms. TN content in CK groups sediment decreased by 0.176 mg/g, it is largely related to the nutrition adsorption from sediment by *V. natans* and microbial metabolism consumption (Lynette et al., 2010; Wang et al., 2018a). Factually, the growth of *V. natans* adsorbs some N and P from water and sediment, and the Al(OH)_3 floc above the sediment forms a barrier to inhibit the release of N and P due to the chelate effect (Hu et al., 2012; Wang et al., 2018b). Sediments TN in 0.3 mg/L and 0.6 mg/L Al^{3+} groups decreased by 0.378 mg/g and 0.260 mg/g respectively from the initial value, which were greater than those treated in NO and CK groups. While sediment TN content in 1.2 mg/L treatments showed no significant difference with NO and CK groups. Al-salt has complexation/passivation effect on nutrient cycle, which will affect the bioavailability of N and P when Al-salt concentration is relatively moderate.

In the CK groups, the sediments IP content decreased significantly after *V. natans* planting, and OP increased significantly. The sediment IP

content in the treatment groups, as well as the Fe/Al-P content in 0.3 mg/L and 0.6 mg/L treatments, decreased significantly comparing with the initial value ($P < 0.05$), however, the Ca-P content didn't significantly change. This suggested that *V. natans* absorbed and utilized some IP for the growth, mainly involving Fe/Al-P rather than Ca-P. IP content accounted for a large proportion of TP, followed by Ca-P, there were significant differences for TP, IP and Fe/Al-P between the initial value and 0.3 mg/L, 0.6 mg/L treatment groups ($P < 0.05$). The slightly reduction of Fe/Al-P in different treatment groups (except for NO groups) may resulted from Eh reduction in rhizosphere sediments, or the trace adsorption and utilization by *V. natans*.

V. natans showed different adsorption capacity of P forms (TP, IP, Fe/Al-P and Ca-P) at different growth stages, and the removal rate of Fe/Al-P was the largest (Wang et al., 2018a). *V. natans* absorbs OP and Fe/Al-P in sediments through mineralization and decomposition, and immobilizes them in plants. Additionally, the coupling processes of metal plaque enrichment of P and oxalic acid complexation of metal could significantly enhance P acquisition by *V. natans* rhizosphere (Xing et al., 2018). The Al(OH)_3 flocs, formed by Al-salts hydrolysis, covered on the sediment surface could also effectively absorb the dissolved P (Reitzel et al., 2005).

3.7. Rhizosphere microbial community variation

As major component of biological decomposers in root ecosystem, rhizosphere microflora play important role in N and P biogeochemical processes (Lynette et al., 2010). The response of microbial community composition under Al-toxicity reflects the transformation of nutrient at the biological level (Zhao and Shen, 2018). Taxonomic composition and cluster trees and histogram of sediment microflora community at genus level are depicted in Fig. 7. 46 main microbe genera in the sediments were detected, there was no significant difference in the microbial community composition, but the significant difference in the relative abundance of the dominant genus was determined.

Citrobacter and *Exiguobacterium* were found to be the dominant genera in all the experimental groups. The maximum abundance of *Citrobacter* (5.04 %) and *Exiguobacterium* (7.86 %) were determined in NO groups, and the minimum abundance (1.95 % and 2.91 %) in CK

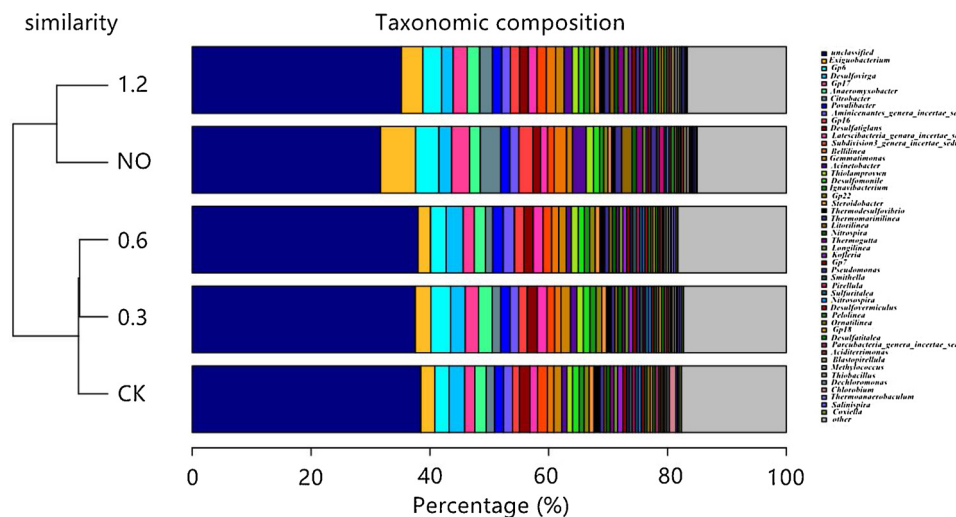


Fig. 7. Taxonomic composition and cluster trees and histogram of rhizosphere microflora community of *V. natans* at genus level in different treatments.

groups. Comparing the NO groups, the abundance of the two dominant genera in treatment groups decreased. While comparing with the CK groups, the abundance of the two dominant genera increased. But the third dominant genus in 0.3 mg/L, 0.6 mg/L and 1.2 mg/L Al³⁺ treatment groups were varied from CK groups and NO groups, which were *Gp6*, *Desulfovibrio*, *Acinetobacter*, *Chlorobiun* and *Acinetobacter*, respectively, accounting for 1.75 %, 2.00 %, 1.99 %, 1.75 % and 3.22 %, there were significant difference among the five experimental groups ($P < 0.05$).

Nitrospira in the phylum Nitrospirae, *Nitrosospira*, *Anaeromyxobacter* and *Aquicella* in Proteobacteria, and *GpXIII*, *GpIX* and *GpIV* in Cyanobacteria were related with the N-transformation process. The abundance percentage of the eight genera (4.72–5.94 %) were significantly varied ($P < 0.05$) among the five experimental groups, indicating a certain variation of some process in N cycle due to the fact that root exudates were changed, and Al³⁺ exerted inhibitory or stimulated effect on the activity of microorganisms (Cooke et al., 2005).

Genera *Dechloromonas*, *Acidovorax* and *Anaeromyxobacter* in the phylum Proteobacteria, *Lactococcus* in Firmicutes, and *Nitrospira* in Nitrospirae, *GP6*, *GP7*, *GP16*, *GP17* and *GP22* in Acidobacteria were the major contributors involved in P cycle (Terashima et al., 2016). The ten genera contributed about 19.34 %, 17.21 %, 18.16 %, 15.93 % and 19.67 % respectively in 0.3 mg/L, 0.6 mg/L and 1.2 mg/L Al³⁺ treatments, CK groups and NO groups. The treatment groups, in which the P removal rate was relatively higher than that of the CK and NO groups, enhanced the function of P metabolism by increasing the abundance of genus *GP6* and *Anaeromyxobacter* (Yuan et al., 2016).

According to the cluster tree, the community composition structure of 1.2 mg/L treatment was similar to that of NO groups, and that of 0.3 mg/L and 0.6 mg/L treatments were similar, then both closed to that of CK groups (Fig. 7). In 1.2 mg/L treatment, the positive effects of *V. natans* on microorganisms may be neutralized by the Al-toxicity, which maybe the reduction of root exudates and radial oxygen loss for *V. natans* root system caused the damage in higher Al³⁺ treatments groups (Kochian, 1995; Ma et al., 2014).

The community diversity was highest in CK groups, followed by that

of 0.6 mg/L treatment, with the lowest in NO groups (Table 2), and the sequence number of microbial community ranked as CK groups > 0.3 mg/L treatment > 0.6 mg/L treatment > NO groups > 1.2 mg/L treatment ($P < 0.05$), which indeed suggested the microbial abundance and composition was affected by both Al-toxicity and *V. natans* growth status.

Comprehensively, Al-salt above a range of concentrations destroyed the submerged plant tissues and rhizosphere microflora, affected the N and P absorption (Huser et al., 2016), and the root exudates and photosynthesis capacity of plants decreased, resulting in the reduction of assimilative substances (Ziae et al., 2014). Therefore, Al-salts, *V. natans* and microflora have a combined effect on N and P in sediment. The N and P nutrition change in these experiment system were significantly correlated with the Al³⁺ concentration, the growth status of *V. natans* and the composition of microbial community in sediments.

Different letters indicate significant differences ($P < 0.05$) among the five treatments. Data represent Means \pm S.E. n=3.

4. Conclusion

The increasing Al concentrations in aquatic systems as a result of anthropogenic interference has exerted greatly stress on submerged plants, involving inhibition on the seeds germination and phytotoxicity on the growth and physiological/biochemical characteristics. Comparing terrestrial plants, the entire individuals of submerged plant *V. natans* suffered Al aquatic-phytotoxicity and root system was one of the important targets of Al-toxicity. The stunted root system and damaged leaves affect plant metabolism by decreasing mineral nutrition and lead to ultimately growth inhibition. The presence of Al plus *V. natans* have synergistic effect on rhizospheric N, P component and microflora community construction. Low dose (< 0.3 mg/L) of Al-salts combined with submerged plants will be more effective not only in controlling N and P load in sediment, but also in improving water quality and sediment microenvironment. The current results displayed that Al-salt affects the growth and propagation of submerged plants and structure of sediment microbial community. Such findings may be

Table 2

The diversity index, organelle number, OTU number of microbial community in control groups and different treatments.

	NO	CK	0.3 mg/L	0.6 mg/L	1.2 mg/L
The Shannon Index	7.08 \pm 0.37 ^c	7.49 \pm 0.45 ^a	7.42 \pm 0.33 ^a	7.46 \pm 0.51 ^a	7.29 \pm 0.31 ^b
The Simpson Index	0.0067 \pm 0.0005 ^a	0.0024 \pm 0.0003 ^c	0.0029 \pm 0.0002 ^b	0.0025 \pm 0.0002 ^c	0.0030 \pm 0.0003 ^b
Organelle number	68 \pm 5 ^d	237 \pm 14 ^a	160 \pm 9 ^b	91 \pm 7 ^c	62 \pm 4 ^d
OTU number	6537 \pm 189 ^b	8218 \pm 217 ^a	8222 \pm 205 ^a	8210 \pm 201 ^a	5939 \pm 193 ^c

practically significant for Al ecological evaluation and scientific utilization, and instructive for the submerged plants restoration in shallow eutrophic lakes with Al input.

CRediT authorship contribution statement

Qingwei Lin: Conceptualization, Methodology, Investigation, Writing - review & editing, Data curation, Funding acquisition. **Mingjun Fan:** Writing - original draft, Investigation. **Xue Peng:** Visualization, Software, Investigation. **Jianmin Ma:** Conceptualization, Methodology, Supervision. **Yi Zhang:** Resources. **Fei Yu:** Software. **Zhenbin Wu:** Project administration, Funding acquisition. **Biyun Liu:** Conceptualization, Methodology, Supervision, Writing - review & editing.

Declaration of Competing Interest

The authors declare that they have no known competing financial interests or personal relationships that could have appeared to influence the work reported in this paper.

Acknowledgments

This work was financially supported by the National Natural Science Foundation of China (31830013), the China Postdoctoral Science Foundation (2019M662498), and the National Key Research and Development Program of China (2019YFA0905503). Lai Wang and Fenli Min, from Institute of Hydrobiology, Chinese Academy of Sciences, were greatly thanked for the field sampling assistance and the data analyses.

References

- Adams, W.J., Cardwell, A.S., DeForest, D.K., Gensemer, R.W., Santore, R.C., Wang, N., Nordheim, E., 2018. Aluminum bioavailability and toxicity to aquatic organisms: introduction to the special section. Environ. Toxicol. Chem. 37, 34–35. <https://doi.org/10.1002/etc.3879>.
- Akram, N.A., Shafiq, F., Ashraf, M., 2017. Ascorbic acid: a potential oxidant scavenger and its role in plant development and abiotic stress tolerance. Front. Plant Sci. 8, 613. <https://doi.org/10.3389/fpls.2017.00613>.
- Bulley, S., Laing, W., 2016. The regulation of ascorbate biosynthesis. Curr. Opin. Plant Biol. 33, 15–22. <https://doi.org/10.1016/j.pbi.2016.04.010>.
- Charlotte, P., Benet, G., Isabel, C., Juan, B., 2008. A glance into aluminum toxicity and resistance in plants. Sci. Total Environ. 400, 356–368. <https://doi.org/10.1016/j.scitotenv.2008.06.003>.
- Chaudhary, M.L., Adu-Gyamfi, J.J., Saneoka, H., Nguyen, N.T., Suwa, R., Kanai, S., El-Shemy, H.A., Lightfoot, D.A., Fujita, K., 2008. The effect of phosphorus deficiency on nutrient uptake, nitrogen fixation and photosynthetic rate in mashbean, mungbean and soybean. Acta Physiol. Plant. 30, 537–544. <https://doi.org/10.1007/s11738-008-0152-0158>.
- Chen, M., Cui, W.T., Zhu, K.K., Xie, Y.J., Zhang, C.H., Shen, W.B., 2014. Hydrogen-rich water alleviates aluminum-induced inhibition of root elongation in alfalfa via decreasing nitric oxide production. J. Hazard. Mater. 267, 40–47. <https://doi.org/10.1016/j.jhazmat.2013.12.029>.
- Collignon, C., Boudot, J.P., Turpault, M.P., 2012. Time change of aluminum toxicity in the acid bulk soil and the rhizosphere in Norway spruce (*Picea abies* (L.) Karst.) and beech (*Fagus sylvatica* L.) stands. Plant Soil 357, 259–274. <https://doi.org/10.1007/s11104-012-1154-2>.
- Cooke, G.D., Welch, E.B., Peterson, S.A., Nichols, S.A., 2005. Restoration and Management of Lakes and Reservoirs, 3rd ed. CRC press, Taylor and Francis, Boca Raton, FL, pp. 616.
- Dawood, M., Cao, F.B., Jahangir, M.M., Zhang, G.P., Wu, F.B., 2012. Alleviation of aluminum toxicity by hydrogen sulfide is related to elevated ATPase, and suppressed aluminum uptake and oxidative stress in barley. J. Hazard. Mater. 209, 121–128. <https://doi.org/10.1016/j.jhazmat.2011.12.076>.
- de Vincente, I., Huang, P., Andersen, F., Jensen, H., 2008. Phosphate adsorption by fresh and aged aluminum hydroxide. Consequences for Lake Restoration. Environ. Sci. Technol. 42, 6650–6655. <https://doi.org/10.1021/es800503s>.
- Doncheva, S., Amenos, M., Poschenrieder, C., Barcelo, J., 2005. Root cell patterning: a primary target for aluminum toxicity in maize. J. Exp. Bot. 56, 1213–1220. <https://doi.org/10.1093/jxb/eri115>.
- Dorea, C.C., Clarke, B.A., 2008. Effect of aluminum on microbial respiration. Water Air Soil Pollut. Focus. 189 (1–4), 353–358.
- He, H.Y., Huang, W.J., Oo, T.L., Gu, M.H., He, L.F., 2017. Nitric oxide inhibits aluminum-induced programmed cell death in peanut (*Arachis hypogaea*L.) root tips. J. Hazard. Mater. 333, 285–292. <https://doi.org/10.1016/j.jhazmat.2017.03.049>.
- Hu, Y.S., Zhao, Y.Q., Zhao, X.H., Kumar, J.L.G., 2012. High rate nitrogen removal in an alum sludge-based intermittent aeration constructed wetland. Environ. Sci. Technol. 46, 4583–4590. <https://doi.org/10.1021/es204105h>.
- Huser, B.J., Futter, M., Lee, J.T., Perniel, M., 2016. In-lake measures for phosphorus control: the most feasible and cost-effective solution for long-term management of water quality in urban lakes. Water Res. 97, 142–152. <https://doi.org/10.1016/j.watres.2015.07.036>.
- Ke, X.S., Li, W., 2006. Germination requirement of *Vallisneria natans* seeds: implications for restoration in Chinese lakes. Hydrobiologia 559, 357–362. <https://doi.org/10.1007/s10750-005-1276-0>.
- Kochian, L.V., 1995. Cellular mechanisms of aluminum toxicity and resistance in plants. Annu. Rev. Plant Physiol. Plant Mol. Biol. 46, 237–260. <https://doi.org/10.1146/annurev.pp.46.060195.001321>.
- Kochian, L.V., Hoekenga, O.A., Pieros, M.A., 2004. How do crop plants tolerate acid soils? Mechanisms of aluminum tolerance and phosphorous efficiency. Annu. Rev. Plant Biol. 55, 459–493 DOI: 10.1146/annurev.aplant.55.031903.141655.
- Kochian, L.V., Pieros, M.A., Liu, J.P., Magalhaes, J.V., 2015. Plant adaptation to acid soils: the molecular basis for crop aluminum resistance. Annu. Rev. Plant Biol. 66, 571–598 DOI: 10.1146/annurev-aplant-043014-114822.
- Kopacek, J., Boroves, J., Hejzlar, J., Ulrich, K.U., Norton, S.A., Amirbahman, A., 2005. Aluminum control of phosphorus sorption by lake sediments. Environ. Sci. Technol. 39, 8784–8789. <https://doi.org/10.1021/es050916b>.
- Lin, J., Sun, Q., Ding, S.M., Wang, D., Wang, Y., Chen, M.S., Shi, L., Fan, X.F., Tsang, D.C.W., 2017a. Mobile phosphorus stratification in sediments by aluminum immobilization. Chemosphere 186, 644–651. <https://doi.org/10.1016/j.chemosphere.2017.08.005>.
- Lin, Q.W., Liu, B.Y., Min, F.L., Zhang, Y., Ma, J.M., He, F., Zeng, L., Dai, Z.G., Wu, Z.B., 2017b. Effects of aluminate flocculant on turion germination and seedling growth of *Potamogeton crispus*. Aquat. Toxicol. 193, 236–244. <https://doi.org/10.1016/j.aquatox.2017.10.029>.
- Lin, Q.W., He, F., Ma, J.M., Zhang, Y., Liu, B.Y., Min, F.L., Dai, Z.G., Zhou, Q.H., Wu, Z.B., 2017c. Impacts of residual aluminum from aluminate flocculant on the morphological and physiological characteristics of *Vallisneria natans* and *Hydrilla verticillata*. Ecotoxicol. Environ. Saf. 145, 266–273 DOI: 10.1016/j.ecoenv.2017.07.037.
- Lin, Q.W., Peng, X., Liu, B.Y., Min, F.L., Zhang, Y., Zhou, Q.H., Ma, J.M., Wu, Z.B., 2019. Aluminum distribution heterogeneity and relationship with nitrogen, phosphorus and humic acid content in the eutrophic lake sediment. Environ. Pollut. 253, 516–524. <https://doi.org/10.1016/j.envpol.2019.07.042>.
- Lynette, M.M.B., John, R.W., Hans, B., 2010. Alum application to improve water quality in a municipal wastewater treatment wetland: effects on macrophyte growth and nutrient uptake. Chemosphere 79, 186–192. <https://doi.org/10.1016/j.chemosphere.2010.02.006>.
- Ma, J.F., Chen, Z.C., Shen, R.F., 2014. Molecular mechanisms of Al tolerance in gramineous plants. Plant Soil 381, 1–12. <https://doi.org/10.1007/s11104-014-2073-1>.
- Morelli, B., Hawking, T.R., Niblick, B., Henderson, A.D., Golden, H.E., Compton, J.E., Cootier, E.J., Bare, J.C., 2018. Critical review of eutrophication models for life cycle assessment. Environ. Sci. Technol. 52, 9562–9578. <https://doi.org/10.1021/acs.est.8b00967>.
- Patricia, S., Manuela, M., 2016. Assessment of the impact of Aluminum on germination, early growth and free proline content in *Lactuca sativa* L. Ecotoxicol. Environ. Saf. 131, 151–156. <https://doi.org/10.1016/j.ecoenv.2016.05.014>.
- Patrick, C.D.H., Grant, D., Anja, V., Ellen, N., Geert, J.B., Benjamin, A.V., Karin, F., Miquel, L., Bryan, S., 2019. Human health risk associated with the management of phosphorus in freshwaters using lanthanum and aluminium. Chemosphere 220, 286–299. <https://doi.org/10.1016/j.chemosphere.2018.12.093>.
- Poschenrieder, C., Gunse, B., Corrales, I., Barcelo, J., 2008. A glance into aluminum toxicity and resistance in plants. Sci. Total Environ. 400, 356–368. <https://doi.org/10.1016/j.scitotenv.2008.06.003>.
- Reitzel, K., Hansen, J., Andersen, F.O., Hansen, K.S., Jensen, H.S., 2005. Lake restoration by dosing aluminium relative to mobile phosphorus in the sediment. Environ. Sci. Technol. 39, 4134–4140. <https://doi.org/10.1021/es0485964>.
- Robert, W.G., Richard, C.P., 1999. The bioavailability and toxicity of aluminum in aquatic environments. Crit. Rev. Environ. Sci. Technol. 29, 315–450. <https://doi.org/10.1080/1064338991259245>.
- Robert, W.G., John, C.G., Patricio, H.R., Jose, J.A., William, A.S., Allison, S.C., Robert, C.S., Adam, C.R., William, J.A., Eirik, N., 2018. Evaluating the effects of pH, hardness and dissolved organic carbon on the toxicity of aluminum to freshwater aquatic organisms under circumneutral conditions. Environ. Toxicol. Chem. 37, 49–60. <https://doi.org/10.1002/etc.3920>.
- Ruban, V., López-Sánchez, J.F., Pardo, P., Rauret, G., Muntau, H., Quevauviller, P., 2001. Harmonized protocol and certified reference material for the determination of extractable contents of phosphorus in freshwater sediments—a synthesis of recent works. Fresenius J. Anal. Chem. 370, 224–228. <https://doi.org/10.1007/s002160100753>.
- Talebi, S., Kalat, S.M.N., Darban, A.L.S., 2014. The study effects of heavy metals on germination characteristics and proline content of triticale (*Triticoseale Wittmack*). Int. J. Farm. Allied Sci. 3, 1080–1087.
- Terashima, M., Yama, A., Sato, M., Yumoto, I., Kamagata, Y., Kato, S., 2016. Culture-dependent and -independent identification of polyphosphate-accumulating Dechloromonas spp. predominating in a full-scale oxidation ditch wastewater treatment plant. Microbes Environ. 31, 449–455.
- Tsakiridis, P.E., 2012. Aluminum salt slag characterization and utilization. J. Hazard. Mater. 217, 1–10. <https://doi.org/10.1016/j.jhazmat.2012.03.052>.
- Vieira, F.C.B., He, Z.L., Wilson, P.C.A., Bayer, C., Stoffella, P.J.A., Baligar, V.C., 2008. Response of representative cover crops to aluminum toxicity, phosphorus deprivation, and organic amendment. Aust. J. Agric. Res. 59, 52–61. <https://doi.org/10.1080/00049430701362001>.

- 1071/AR07120.
- Wang, X.B., 2010. Study on the Influence of Aluminum Salt on Microbial Community and Contaminant Removal in Activated Sludge. Xi'an university of architecture and technology, Xi'an, pp. 30–36.
- Wang, C., Liu, Z.S., Zhang, Y., Liu, B.Y., Zhou, Q.H., Zeng, L., He, F., Wu, Z.B., 2018a. Synergistic removal effect of P in sediment of all fractions by combining the modified bentonite granules and submerged macrophyte. Sci. Total Environ. 626, 458–467. <https://doi.org/10.1016/j.scitotenv.2018.01.093>.
- Wang, C.H., Wu, Y., Bai, L.L., Zhao, Y.Q., Yan, Z.S., Jiang, H.L., Liu, X., 2018b. Recycling of drinking water treatment residue as an additional medium in columns for effective P removal from eutrophic surface water. J. Environ. Manage. 217, 363–372. <https://doi.org/10.1016/j.jenvman.2018.03.128>.
- Wei, J.Y., Yao, N., Lai, Z.Q., Lai, D.W., Qiu, J.H., Deng, S.Y., 2013. Seed germination characteristics of *Stybsanthes guianensis* cv. under different drought stress. J. Southern Agric. 44, 1977–1980. <https://doi.org/10.3969/j.issn.2095-1191.2013.12.1977>.
- Xing, W., Wu, H.P., Hao, B.B., Huang, W.M., Liu, G.H., 2013. Bioaccumulation of heavy metals by submerged macrophytes: looking for hyperaccumulators in eutrophic lakes. Environ. Sci. Technol. 47, 4695–4703. <https://doi.org/10.1021/es303923w>.
- Xing, X.G., Ding, S.M., Liu, L., Chen, M.S., Yan, W.M., Zhao, L.P., Zhang, C.S., 2018. Direct evidence for the enhanced acquisition of phosphorus in the rhizosphere of aquatic plants: a case study on *Vallisneria natans*. Sci. Total Environ. 616, 386–396. <https://doi.org/10.1016/j.scitotenv.2017.10.304>.
- Yamamoto, Y., Kobayashi, Y., Devi, S.R., Rikiishi, S., Matsumoto, H., 2002. Aluminum toxicity is associated with mitochondrial dysfunction and the production of reactive oxygen species in plant cells. Plant Physiol. 128, 63–72. <https://doi.org/10.1104/pp.010417>.
- Yu, Y., Jin, C.W., Sun, C.L., Wang, J.H., Lin, X.Y., 2015. Elevation of arginine decarboxylase-dependent putrescine production enhances aluminum tolerance by decreasing aluminum retention in root cell walls of wheat. J. Hazard. Mater. 299, 280–288. <https://doi.org/10.1016/j.jhazmat.2015.06.038>.
- Yu, Q., Wang, H.J., Wang, H.Z., Li, Y., Liang, X.M., Xu, C., Jeppesen, E., 2017. Does the responses of *Vallisneria natans*(Lour.) Hara to high nitrogen loading differ between the summer high-growth season and the low-growth season? Sci. Total Environ. 601, 1513–1521. <https://doi.org/10.1016/j.scitotenv.2017.05.268>.
- Yuan, Y., Liu, J., Ma, B., Liu, Y., Wang, B., Peng, Y., 2016. Improving municipal wastewater nitrogen and phosphorous removal by feeding sludge fermentation products to sequencing batch reactor (SBR). Bioresour. Technol. 222, 326–334. <https://doi.org/10.1016/j.biortech.2016.09.103>.
- Zhao, X.Q., Shen, R., 2018. Aluminum-Nitrogen interactions in the soil-plant system. Front. Plant Sci. 9, 1–15. <https://doi.org/10.3389/fpls.2018.00807>.
- Zhou, X.H., Gu, Z.H., Xu, H.N., Chen, L.M., Tao, G.X., Yu, Y.X., Li, K.Z., 2016. The effects of exogenous ascorbic acid on the mechanism of physiological and biochemical responses to nitrate uptake in two rice cultivars (*Oryza sativa* L.) under aluminum stress. J. Plant Growth Regulat. 35, 1013–1024. <https://doi.org/10.1007/s00344-016-9599-9>.
- Ziae, N., Rezaiatmand, Z., Ranjbar, M., 2014. Study of aluminum toxicity on photosynthetic pigment, soluble sugars and proline contents in two sunflower varieties. Res. Crop Ecophysiol. 9, 105–113.
- Zuo, J.C., Liu, L.D., Kong, D.R., Zhang, S.M., Hu, D.C., Xie, W.H., 2016. Effects of sediment burial on seed germination and seedling establishment of *Vallisneria natans*. J. Freshwater Ecol. 31, 289–297. <https://doi.org/10.1080/02705060.2015.1116469>.